# Three-dimensional modelling of injection moulded micro structured optical components.

**Bachelor Thesis**
**Alberto García Martínez - s186461**

**Supervisors**
**Guido Tosello - Associate Professor**
**Dario Loaldi - Phd Student**

Technical University of Denmark
Bachelor Thesis
June 11, 2019

**Department of Mechanical Engineering**
Section of Manufacturing engineering
Danmarks Tekniske Universitet
Produktionstorvet Building 427
DK-2800 Kgs. Lyngby
Denmark
www.mek.dtu.dk
Tel: (+45) 45 25 19 16
Fax: (+45) 45 93 14 75
Email: info@mek.dtu.dk

Abstract

Fresnel lenses are widely used in many industrial fields involving light concentration due to its versatility and compact size. Their functioning principle is well studied and they can be easily obtained by injection molding for a low price. Being optical components, Fresnel lenses have to be manufactured using a high precision methods in order to meet its tight geometrical tolerances.

Micro structured optical components such as Fresnel lenses, are difficult to model using commercial software. Microscopic features' size can not be replicated easily with most simulating tools and virtual models have. In order to optimize the manufacturing procedures and obtain better quality parts, the process needs to be simulated. Simulation is nowadays an indispensable tool for designers and there is a need to improve three dimensional models of micro structured plastic parts.

During this report, a three dimensional model of a micro structured optical component is to be obtained using Autodesk's Moldflow simulation software. The model has to be validated by comparing data from the simulations with injection molded pieces.

# Preface

This report summarizes the work of nearly four months developing and validating a three-dimensional model of injection moulded optical components. From February to June 2019, I have been able to learn about injection molding and how simulation software is used to improve part design and manufacturing processes, both new topics to me.

The Bachelor Thesis represents the end of my bachelor degree in mechanical engineering, which I have been studying for the last few years at my home university, the Universitat Politècnica de València. Having the opportunity of doing my thesis at DTU as an exchange student inside the European Union's Erasmus+ program, has enriched myself in many different ways. During my stay here, I have been able to learn from an international environment, being able to experience new learning methods and a new work discipline.

Thank you to my supervisors Dario and Guido and to everybody who has helped me to be here.

# Contents

# 1 Introduction

The aim of this project is to build and validate a three-dimensional model of micro-structured optical components produced using injection moulded polymers. To simulate the injection moulding process, the commercial software Moldflow will be used.

Parts to be modelled are Fresnel lenses, a kind of compact lens used in many fields involving light concentration. Even Fresnel lenses are macroscopic, they usually contain microscopic elements that must also be modelled. This makes an accurate digital twin of the process difficult to obtain, as no commercial software is able to precisely mimic the influence of both microscopic and macroscopic features. Therefore, some special considerations have to be taken into account when creating the model using Moldflow. All this considerations will be further explained in this report while studying the requirements and limitations of modelling at micro and sub-micro scale.

The main objectives of this projects can be listed as:

- Studying injection compression molding for high precision manufacturing.
- Obtaining a digital model of the injection process using commercial software.
- Observe how modifying injection conditions affects the results.
- Validate the model by comparing it with injection moulding experiments.
- Quantify the differences between simulations and injection moulding experiments.

For an adequate validation of the model, not only injection parameters are to be compared, but also geometrical characteristics of the real pieces and the simulations together with a comparison of the real; simulated and theoretical mass of the pieces. Adequate measurement instruments have to be selected for both geometrical and mass comparison.

## 1.1 Fresnel lenses

Fresnel lenses are a a type of compact lens composed by many annular stepped zones. Even stepped lenses were first described by Georges de Buffon in the XIIX century, this multi-part lens technology was highly developed by French physicists Agustin-Jean Fresnel in early XIX century. [1]

Normal spherical lenses become thicker when augmenting their diameter with a fixed focal length. As the refraction causing light concentration only occurs when the light enters a different medium, the only part of a traditional lens that is essential for its proper function is the border between the glass and the air. By removing the material that is not essential, concentric annular sections are obtained. Each of this sections can be reduced in thickness as long as the resulting step has the same surface curvature as the continuous lens. This way, the overall thickness of the lens is significantly reduced, making it lighter and more compact. [2]

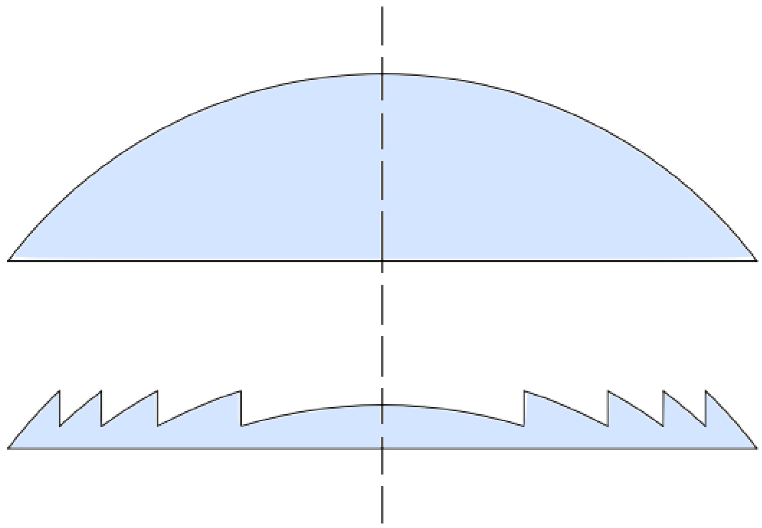

**Figure 1** | Cross section of a traditional spherical lens and its equivalent Fresnel lens - **Produced in Inkscape**

Due to its thin size, Fresnel lenses are used in many industrial fields involving light concentration, from photography and imaging to the automotive industry. One remarkable use of this lenses is as solar concentrators for photovoltaic energy generation.

Even traditionally made out of glass, Fresnel lenses can be produced by injection molding. Avoiding the use of glass, it is possible to obtain lighter and cheaper lenses. Polymeric lenses can be mass produced, but they still have to meet tight tolerances for an adequate performance. Not only geometrical tolerances have a big impact in the lens performance; it has been observed that some double refraction effects are linked to high stress levels in the piece during production.

The dual structure of Fresnel lenses and its precision requirements, makes it essential to be in tolerance both at meso and micro scale. Optical level roughness, sharp peak radius or an adequate ridge height are some examples of microscopic level parameters that affect the performance of the piece. [3] [4]

Simulating the injection molding process makes it possible to predict filling errors that can affect the optical properties of the lens. Therefore, a good digital model of the process can assure that the tolerances mentioned above are within their tight limits, allowing to adjust injection conditions to optimum levels before starting production. The complex structure of Fresnel lenses requires multi-scale simulations as a way to precisely replicate the plastic flow behaviour at any point. This simulation procedure will be further explained on this report.

## 1.2 Injection compression molding

Polymer components are widely produced using injection molding techniques. This replication procedures generally consists of three basic phases: plastification, injection and cooling and ejection. Injection compression molding is the method chosen for the injection experiments and, as a variant of the classic procedure, it also follows the previous steps

The injection phase is crucial for obtaining a piece that meets the quality requirements of a Fresnel lens. It is also the phase to be modeled on this thesis and it is divided in three sub-phases. Given the importance of the injection phase on this project, its three stages are explain as follows. [5]

1. **Filling:** The molten polymer is pushed by a ram moving at a steady speed inside the mold cavity. The ram moves this way until the cavity is just filled.
2. **Pressurization:** Molten plastic is a compressible fluid. The ram would not stop moving forward just when the mold is filled, but it will take it some time to stop. In the meantime, plastic will continue flowing into the mold, augmenting the pressure inside the cavity. During this phase, up to an extra 15% volume of material can be forced into the cavity.
3. **Compensation:** Plastic suffers a volumetric change when it cools down and solidifies inside the mold. This change tends to be of around 25% and therefor is larger than the usual volume of plastic injected during the pressurization phase. In order to compensate this volume change and completely fill the cavity, more material is injected inside the cavity.

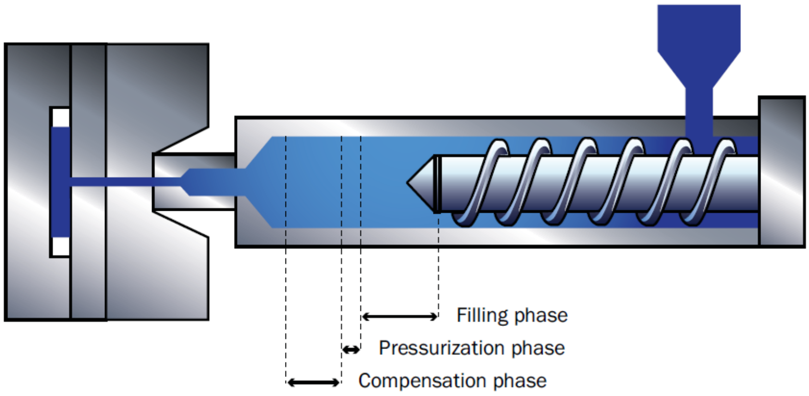


**Figure 2** | Phases of injection - **Picture from Moldflow design guide** [5]

Injection compression molding is a variant of the basic injection molding procedure. This technique is the state of the art technology for molding mass produced optical components. In a basic injection molding machine, the melt polymer flows into the mold following the geometry of the cavity and surpassing the constrains that it creates. This can lead to high stress levels, specially during the pressurization phase, as the polymer is compressed against this cavity constraints. As mentioned before, it is known that high stress levels are linked to birefrigerence problems. Injection compression molding reduces stress levels during injection, making it possible to obtaining better quality pieces.

By adding a new stage to the traditional procedure, injection compression molding ensures a more homogeneous replication of the part. This phase is called compression stage and takes place just after the injection phase. During the injection process, the polymer is injected into the cavity freed from clamping forces, being the cavity thicker than the nominal thickness of the part. This can be done by leaving a small gap between the two parts of the mold, known as compression gap, that makes the melt flow less dependant on the cavity geometry. This freed melt flow makes polymer chain distribution more homogeneous inside the cavity, which improves birefrigerence quality in optical components. Once the cavity is completely filled, it is compressed by a normal force, closing the compression gap and reducing its thickness to the nominal thickness of the part. This last part is the compression stage[6] [7]

# 2 State of the art

Digital modelling of manufacturing processes has become an essential part of engineering. Injection molding simulation software has been used since the late 70's and it is a well established tool in the plastic manufacturing industry. By digitally recreating the molding process, it is possible to improve both the part and the process design, ensuring better quality pieces with less experimental trials.

Simulation has many different benefits when designing injection molded parts. It helps designers foresee production problems before making any mold trial and allows to establish and acceptable processing window without having to rely too much on empirical experience or injection trials. By simulating the process it is possible to predict filling errors such as hesitations, weld lines or cavity unbalances that affect the part quality. Current simulation tools have shown to be effective when modeling most kind of pieces, but modeling multi-scale and micro-scale pieces can be challenging and more in depth studies have to be done. [8]

Fresnel lenses have both micro and macro-scale features, and are this micro-scale features what make theme interesting for this study. Fresnel lenses have been chosen in many previous researches trying to obtaining three dimensional models of injection molded micro structured pieces. Having many applications in industry, a well studied geometry and a multi-scale structure, they are a good sample to be modelled.[9]

The micro-scale features of Fresnel lenses cause two major problems when simulating the injection molding process. Firs of all, some physical phenomena that are irrelevant at a macroscopic scale can have an impact on the plastic flow at microscopic scale. This physical aspects includes surface tension, microrheology or wall slip. The second problem for simulating micro structured components is the multi-scale nature of the piece itself, specifically in the obtention of an adequate mesh to accurately reproduce the piece geometry. As commercial software is used, there is no control over the assumptions that it makes for solving the equations. All the efforts will therefore be focused on obtaining a good quality mesh, as it can be modified with nearly no limitations. [10]

Having both macroscopic and microscopic features in the same piece causes an important dilemma when creating the mesh. Meshing the pat only with small elements would assure a proper reproduction of the geometry, but would also make the model more complex, consuming more computational power and taking more time for obtaining a solution. On the other hand, a rough mesh would only recreate the macroscopic features, not replicating the microscopic ones. The solution implies creating a mesh which elements become smaller when approaching the microscopic features. More information about the method followed to do generate the mesh will be given further in this report.

Validation of the model has also to consider the micro structure of the piece and its singularities. Meso-scale validation will be based in injection parameters, mass, and dimensional comparisons between the model and the pieces from the experiments. Microscopic validation would imply dimensional comparisons of the microscopic features between the model results, the injected pieces and the nominal values of the piece. This last comparisons couldn't be done due to time concerns so only macroscopic scale validation was performed. Appropriate measurement tools and data analysis techniques were chosen in order to validate the model at meso-scale.

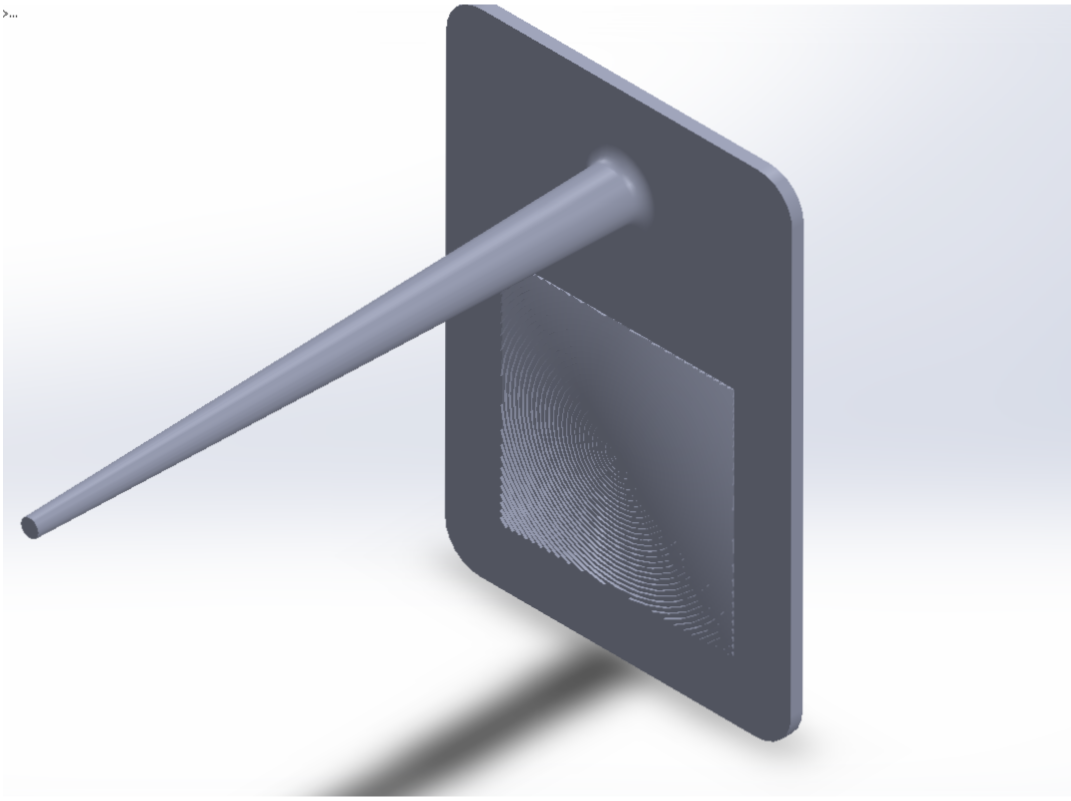

**Figure 3 |** Isometric view of the Fresnel lens - **Picture from Solidworks**

# 3 Materials and instrumentation

In order to build and validate the model, different materials and instrumentation had to be used. A list of materials used in the project together with an explanation of theme and their influence to the project will be developed on thins section, registering them in no particular order.

## 3.1 Moldflow simulation software:

The model was obtained using Moldflow, a commercial solution form Autodesk Corporation for plastic injection and compression mold simulation. The version used during the project was Moldflow Insight 2017. It was chosen due to its availability, together with its user oriented interface. The sofware is designed so that it is intuitive to use while being able to precisely simulate the injection process. This plays a key role in the software choice, as it allows the user to learn how to use the program within a reasonable time, beeing able to meet the thigh deadlines of a thesis like this.

**Figure 4 |** Moldflow insight 2017 logo. **Picture from Autodesk Moldflow Insight Advanced Flow Practice Manual [11]**

Moldflow uses finite element analysis for modelling three dimensional filling behaviour of a mold design. It solves equations for conservation of mass, momentum and energy together with the stress tensor, that includes equations for modeling the non-Newtonian behaviour of the polymer. This solving method is known as weak problem formulation and it is one of the main techniques for finite element analysis problems. The mathematical model also includes gravity, compressibility and inertial stress. [9] [12] [11]

## 3.2 Injection molded Fresnel lenses:

The experimental pieces where given by the supervisors. They formed a batch of injection molded pieces in different short shots. The concept of short shot will be explained further in this report. The design is of a square Fresnel lens of (40 x 40 $mm$) embedded in a larger rectangular frame of (60 x 82 x 2 $mm$). The lens is radially symmetric with respect to the optical axis with its center at 40 mm from the gate center. The nominal grooves pitch angle is 2°, the depth of the grooves increases from 17.3 $\mu m$ up to 346.8 $\mu m$ radially from the optical axis. The pitch separating each groove is constant and equal to 748.1 $\mu m$.

## 3.3 Zeonex E48R:

The pieces were molded using Cyclo Olephin Polymer (COP) commercially available with the name Zeonex E48R from Zeon Europe GmbH. It is a high quality transparent plastic primarily used for optical components. The variety E48R is chosen because of its high transparency, low water absorption, low birefringence, high heat resistance and superior moldability. [13]

Cyclo Olephin Polymer is an amorphous polymer. Its properties are summarized in the next figure and table.

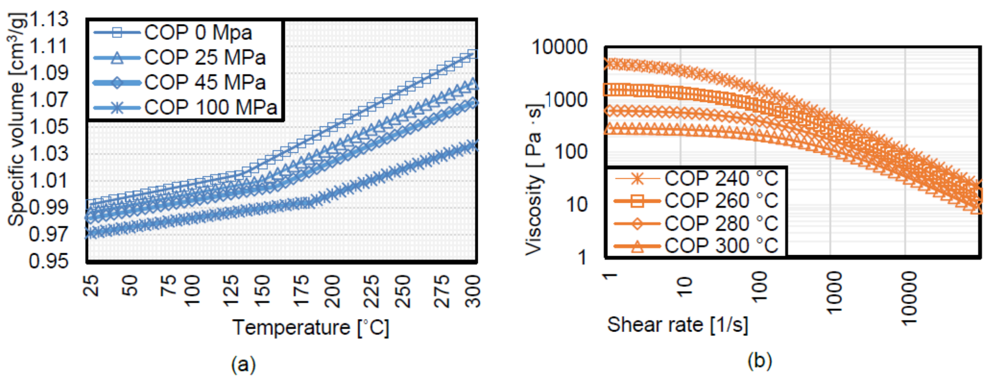


**Figure 5** | COP properties within the process conditions: pvT (a) viscosity (b). **Graphs from: Modelling the filling behavior of micro structured plastic optical components [9]**

**Table 1** | COP principal properties. **Data from Zeon website [13]**

| Propertie | Value | Units |
|---|---|---|
| Elastic modulus ($E_1$) | 2820 | MPa |
| Elastic modulus ($E_2$) | 2330 | MPa |
| Poissons ratio ($\nu_{12}$) | 0.36 | |
| Poissons ratio ($\nu_{12}$) | 0.47 | |
| Shear modulus ($G_{12}$) | 1130 | MPa |
| Melt density | 0.91893 | $g/cm^3$ |
| Solid density | 1.0074 | $g/cm^3$ |

## 3.4 Injection machine:

All the pieces where given at the begining of the thesis so no injection experiments were done during the period covered by this project. Essential information of the machine was also given with the pieces so simulation could be programmed properly.

The machine used for injecting the pieces is the Negri Bossi V70-180. This machine features a 32 $mm$ diameter screw and is capable of a maximum claping force of 600 $kN$. All the injection molding data was obtained using the sensors included in the machine. Time versus Screw Position and Time versus Pressure at injection point curves were given for every piece produced with data obtained from the machine.

## 3.5 Optical coordinate measuring machine:

Measurements with an optical coordinate measuring machine (optical CMM) where done trying to obtain data for the meso-scale verification of the model. The optical CMM used for this measurements was the De Meet 220 manufactured by dutch company Schut Geometrical Metrology. This machine has a measuring range of (220 x 150 x 100 $mm$) and with a resolution of 5 $\mu m$ and an X-Y accuracy of $4 + L[mm]/150\mu m$.

With the optical CMM it was intended to measure as much macroscopic features as possible, specially the fresnel lense square (both width and lenght) the sprue diameter and the diameter of some of the ridges. Altough it seemed an apropiate machine for making the measurements, the piece geometry made it difficult to measure it as the machine was not able to properly detect the lines defined by the contours of the features. Measurements were dropped down due to replication problems, having deviations of up to 60% between measurements in some cases.

## 3.6 Digital Scale:

For the meso-scale verification of the model, mass comparisons between the simulated, the real pieces and the effective nominal mass of the piece were done. Injection molded pieces had to be weighted using a digital scale, and more specifically, a Shimadzu AW220. This machine has a weighting range defined between 10 $mg$ and 220 $g$ with a definition of 0.1 $mg$ and an error of 1 $mg$. It is therefore an adequate scale to weight pieces that are around 10 $g$ as the Fresnel lenses used in this thesis. All the short shots and the completed parts were weighted with the sprue.

## 3.7 Micrometer and Caliper:

For measuring macroscopic features of the pieces and compare theme with their nominal values, pieces were measured using a micrometer and a digital caliper. The caliper is digital, with a resolution of 0.01 $mm$ and a range of measurement that goes from 0 $mm$ to 150 $mm$.The micrometer has a resolution of 0.01 $mm$ and a measure range of 0 $mm$ to 25 $mm$. Measurements of the piece thickness were taken using the micrometer whereas length, width and sprue diameter were measured with the caliper. By measuring the pieces it is possible to verify if they have been replicated according to the nominal values during the injection process.


**Figure 6** | Picture of the caliper used to measure the pieces. **Photograph by the author.**

## 3.8 Calibration gauge blocks:

All measurements have to be expressed with their uncertainty. For ensuring a good uncertainty budget, both the micrometer and the caliper were calibrated before taking the measurements. The gauge blocks used to calibrate the instruments are Grade 2, with calibration certificate number 011811 and following the standard DIN-861.

The micrometer was calibrated using a 2 $mm$ gauge block with a deviation of +0.2 $\mu m$ according to the calibration certificate. The caliper was calibrated two times, one with a 60 $mm$ gauge block that has a deviation of +0.55 $\mu m$ and a second time using an 8 $mm$ block with +0.3 $\mu m$ according to the certificate.

**CERTIFICATE OF INSPECTIOCN**
**GAGE BLOCKS**

MAKE
TYPE RECT
STANDARD DIN861
DATE Aug 20 2001
SET NO 011811 47pcs
GRADE 2
MATERIAL STEEL
MKØ1.

Deviation from nominal size in

| Nominal Size (mm) | Identification No | Deviation (μ m) | Nominal Size (mm) | Identification No | Deviation (μ m) | Nominal Size (mm) | Identification No | Deviation (μ m) | Nominal Size (mm) | Identification No | Deviation (μ m) |
|---|---|---|---|---|---|---|---|---|---|---|---|
| 1. 005 | 01404 | +0. 2 | 1. 12 | 00035 | +0. 14 | 1. 6 | 01487 | −0. 28 | 9 | 01164 | +0. 2 |
| 1. 01 | 01465 | +0. 15 | 1. 13 | 01200 | +0. 2 | 1. 7 | 00456 | −0. 03 | 10 | 01275 | +0. 28 |
| 1. 02 | 01989 | −0. 15 | 1. 14 | 01324 | +0. 15 | 1. 8 | 01352 | +0. 4 | 20 | 01567 | −0. 35 |
| 1. 03 | 00492 | −0. 35 | 1. 15 | 01200 | +0. 1 | 1. 9 | 00542 | −0. 3 | 30 | 00292 | −0. 3 |
| 1. 04 | 00857 | +0. 25 | 1. 16 | 00529 | −0. 22 | 1 | 01396 | −0. 25 | 40 | 01481 | −0. 6 |
| 1. 05 | 01238 | +0. 25 | 1. 17 | 00044 | +0. 32 | 2 | 01140 | +0. 2 | 50 | 01035 | −0. 15 |
| 1. 06 | 01164 | +0. 22 | 1. 18 | 01293 | −0. 1 | 3 | 01846 | −0. 2 | 60 | 00258 | +0. 55 |
| 1. 07 | 01124 | +0. 18 | 1. 19 | 01125 | −0. 2 | 4 | 00114 | −0. 22 | 70 | 01372 | −0. 25 |
| )8 | 01671 | +0. 2 | 1. 2 | 01391 | −0. 32 | 5 | 01029 | +0. 18 | 80 | 01105 | +0. 82 |
| 1. 09 | 00451 | −0. 3 | 1. 3 | 01483 | +0. 2 | 6 | 01557 | +0. 42 | 90 | 01314 | +0. 03 |
| 1. 10 | 01385 | 0 | 1. 4 | 01194 | +0. 23 | 7 | 01520 | +0. 22 | 100 | 01806 | +0. 8 |
| 1. 11 | 00654 | −0. 1 | 1. 5 | 01626 | −0. 42 | 8 | 01498 | +0. 25 | | | |

REMARKS: Standard reference temperature: 20°C(68°F)
Coeffcient of thermal expansion: $(11.5\pm1.0)\times10^{-6}/°C$
INSPECTOR L-05

**Figure 7** | Calibration certificate of the gauge blocks. **Scanned copy of the original at DTU Metrology Lab.**

# 4 Simulation Setup

On this section, the method used to obtain a model of the Fresnel lens will be explained. As mentioned in section (2), using commercially available software implies having no control over the equations that are used to simulate the filling behaviour or the assumptions the software does to solve this equations. In order to obtain a good quality model, an adequate mesh has to be constructed as it can be modified and has a big impact in the final results. An explanation on the simulations that were performed to validate this model is also to be explained.

## 4.1 Meshing in Moldflow:

Every finite element analysis software uses a finite element mesh, commonly referred simply as mesh, to run the analysis. A mesh is formed by a group of elements that divide the geometry of the piece to be simulated in smaller domains. The elements are defined by nodes, which represent coordinates in space limiting the region (that can be 2D or 3D) defined by the element.

The equations that model the filling behaviour of the part are defined and solved for each element. The unknown factors defined as mathematical functions become the value of this functions on the nodes. The behaviour inside of the elements is defined based on the nodal results using interpolation equations. Once the model is solved for each element, the solution of the hole system is obtained by assembling the elements.

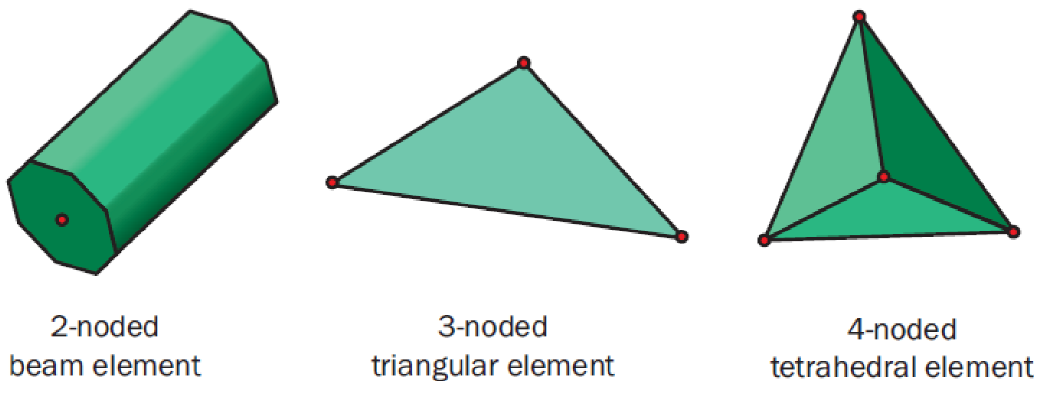


**Figure 8** | Element types in Moldflow. **Picture from Moldflow Design Guide [5]**

There are many different types of finite elements for meshing parts. They can be classified depending on their shape and number of nodes. When using Moldflow, three kinds of elements can be utilized: Linear beam elements, only used to describe parts like feed systems that are not features of the piece; linear triangular elements and linear tetrahedral elements. Triangular and tetrahedral elements are associated with different types of mesh. Moldflow mesh types are listed below: [5]

1. **Midplane:** This kind of mesh uses triangular elements to describe the piece. The mesh is defined in the center line of the plastic cross section and a thickness property is assigned to it. For obtaining good results, the piece has to have a width to thickness ratio lower than 4:1 as higher ratios would cause high error values in the simulation.

2. **Dual domain:** Triangular elements are defined on the surface of the plastic cross section. The distance between elements in opposite sides of the piece defines its thickness. The mesh density becomes more important for achieving high accuracy. The percentage of matched elements in a dual domain mesh, determines the quality of the mesh.

3. **3D mesh:** As it is deduced from its name, this mesh uses tetrahedral elements. Several rows of this elements are stack to define the cross section of the piece. Fewer assumptions are made for solving the problem. Full 3D Navier-Stokes equations are used by the solver. Pressure, temperature and the three velocity components are obtained for each node. Heat conduction is considered in every direction and inertia and gravity effects can also be considered.

### 4.1.1 Mesh requirements

With all the information that has yet been exposed on this report, it is possible to summarize the requirements that the mesh used in the model should have. Taking into account the micro-structure of Fresnel lenses together with the need of an good model that can ensure the high quality standards of the pieces, the next lists of requirements have to be met:

- The mesh has to be fine enough to accurately mimic the microscopic features but without using too small elements so that no excesively long calculation times and high computation power are needed.

- For correctly recreating the smallest features, the mesh has to be no larger than 2.5 $\mu m$. This way, we ensure

- Given the nature of Fresnel lenses as optical components, simulation should have the lowest error possible. For reaching this precision requirements, the usage of a 3D mesh is needed. This mesh takes into consideration more physical phenomena.

### 4.1.2 Limitations of modeling in Moldflow

Moldflow is designed for simulating the filling behaviour of macroscopic pieces. It does not have into account possible size effects commonly seen in microscopic features like capillarity or an increase in the heat flow transferred from the piece to the mold. Modelling all this effects would imply special boundary conditions that are either impossible or really difficult to implement in Moldflow. Being friendly user oriented makes the software be sometimes limited in the customization capabilities.

Going back to the finite elements mesh, some limitations are also found in Moldflow's meshing engine. The minimum element size generated by Moldflow is 0.01 $mm$. As it has been said before, the optimum element size should not be larger than 2.5 $\mu m$ for the smallest features. Automatic generated meshes are not fine enough for recreating the smallest features so it has to be manually adjusted. Large regions with small element sizes take a considerable amount of time to mesh, measured in days and sometimes taking up to a week.

As a way to avoid meshing limitations in Moldflow, trials were made using other finite element analysis software to obtain the mesh. The idea was to obtain a dual domain mesh with the optimal characteristics and then export it to Moldflow where it would be transformed into a 3D mesh. Obtaining 3D meshes from dual domain meshes is a common process as it makes the 3D meshing process faster and allows to perform possible corrections in an easy way on the dual domain mesh. However, a problem was encountered when obtaining the 3D mesh from the imported dual domain mesh. Connectivity problems were found, meaning that the piece was not treated as a hole connected entity but as two separated bodies. The piece was also tried to be imported directly in 3D from another software, but this option had to be rejected as it was taking too much computational power and time.

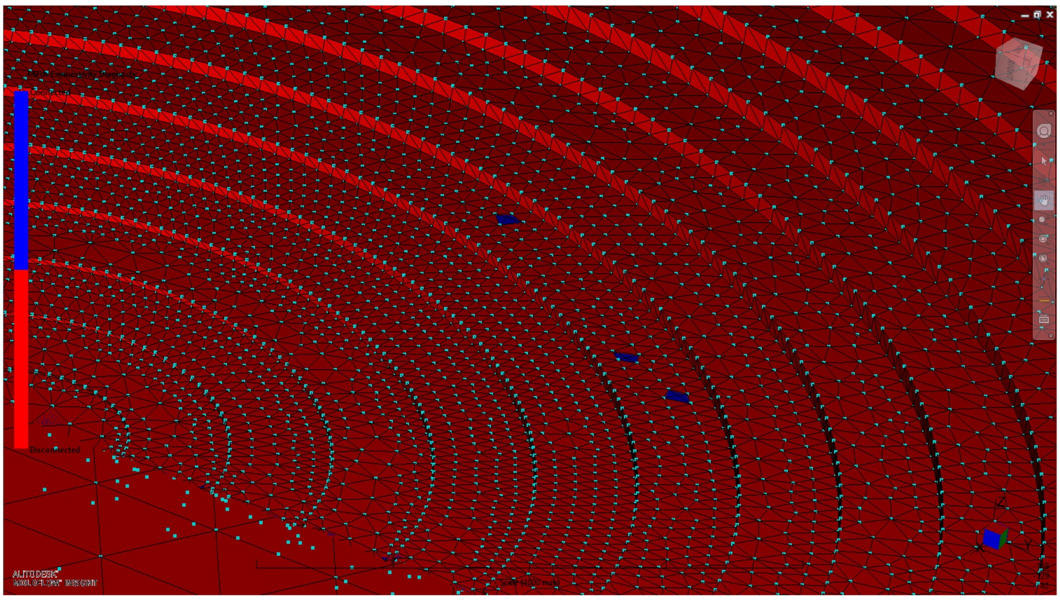

**Figure 9** | Detail of the connectivity analysis. Each colour represents a connectivity region. **Picture from Moldflow**

## 4.2 Obtention of the Mesh

As it has been mentioned before in this report, meshing is the most important part when modelling micro-structured optical component using commercial software. Correctly representing the geometry of both macroscopic and microscopic features assures obtaining good results from the simulations. Types of meshes and Moldflow limitations on obtaining a good model have been discussed previously. The solution to overcome this problems obtaining a good model is explained in this point.

The first step for obtaining the mesh was producing a dual domain mesh using Molflow's meshing tool. Element size was determined to be 1 $mm$ so that every macroscopic feature was represented in detail. It was verified that the dual domain mesh had no issues such as bad connectivity, free edges or high aspect ratios. This was checked using the mesh diagnostic tool featured on Moldflow.

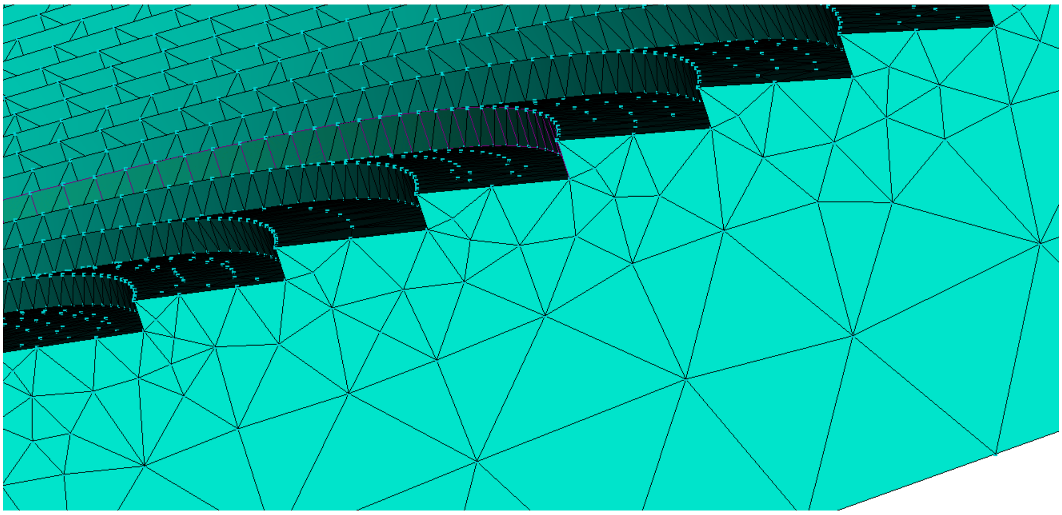

**Figure 10** | Cross section of the part after the first 3D mesh was obtained. **Picture from Moldflow Insight 2017**

The dual domain mesh was transformed into a 3D mesh by using the advancing front method in both surfaces and thickness of the piece. Element size at this point is not fitting for microscopic features so the mesh has to be refined. On a first attempt, local refinement was tried to be done using concentric regions with element size decreasing when approaching to the center of the lens. This technique did not show good results as regions for smallest features, and therefor smaller size elements, were too big and took too much time to mesh.

As the smallest element size in Moldflow is 10 $\mu m$, which is bigger than the 2.5 $\mu m$ needed; and ridge 14 was suggested as the control area for the micro-scale validation, efforts were put in refining the mesh around this ridge. The objective was to reach the minimum element size at a small region around this ridge without having to use too much computational power or creating elements with a high aspect ratio. Rectangular shape regions where defined around ridge 14 one into another. Their shape was thinner and shorter the nearest the rectangle was from the center. Element size was decreased until reaching 10 $\mu m$ at the control ridge, always limited by a maximum growth rate of 1.5 to minimize the risk of high aspect ratio elements.

Size of the rectangular shape regions, embedded one into the other, made it possible to obtain a mesh that gradually refined when approaching the control ridge. The area for doing this was small enough so it would not take much time and power to mesh while ensuring good definition results in ridge 14. A table with the mesh statistics can be seen below.

**Table 2** | Mesh statistics. **Data from Moldflow Insight 2017**

| **Parameter** | **Value** | **Units** |
|---|---|---|
| Element type | Tetra. | |
| Cavity Volume | 13.275 | $cm^3$ |
| Meshed Volume | 13.275 | $cm^3$ |
| Max aspect ratio | 271.39 | |
| Min aspect ratio | 1.02 | |
| Avg aspect ratio | 3.93 | |
| Number of elements | 3248186 | u |
| Connected nodes | 598028 | u |
| Conectivity regions | 1 | u |

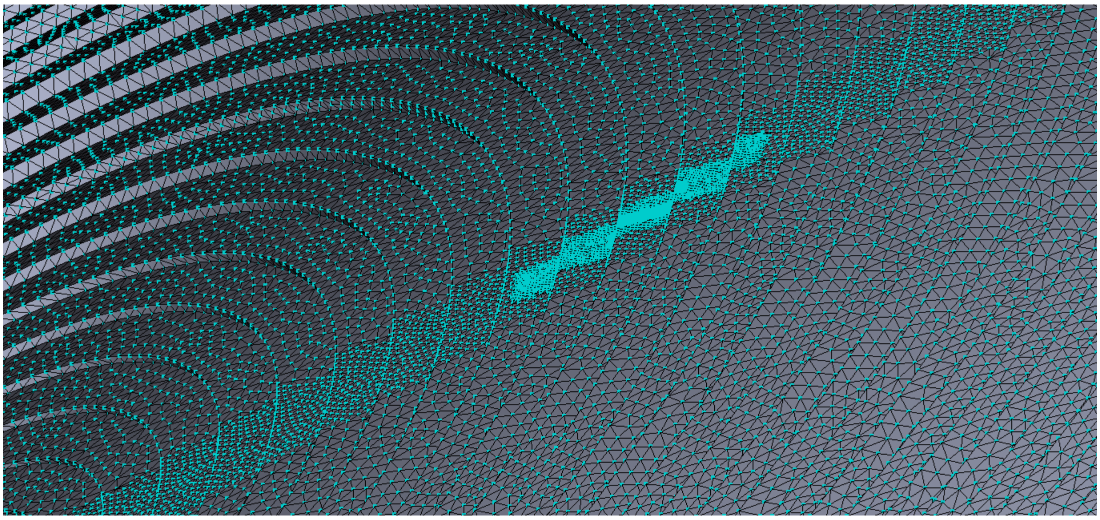

**Figure 11** | Detail of the mesh at ridge 14. It is possible to see how the elements get smaller when approaching the ridge. **Picture from Moldflow Insight 2017**

## 4.3 Modelling experiments

Validating the model implies executing a series of simulations with different injection conditions that can confirm that the digital twin behaves as expected. By changing some of the injection conditions and studying how they affect the final results, it is possible to see how much do they deviate from the real values and determine the influence of each of them on the simulation. Some of the input parameters are changed, maintaining constant the others. They are chosen according to what is expected to affect more the final results.

The simulation experiments are programmed following a three level full factorial design. This means that three different parameters are changed between three different values, leading to 27 combinations to be simulated. The settings to be changed are the ram speed, the melt temperature and the venting. Melt temperature and ram speed are simulated with the value used to program the injection machine as well as with one value slightly above and one immediately below. As no data for the venting was given, three values were chosen based on typical values of mould roughness as a way to study how it can affect the results. It is possible to see the values to be combined in the next table.

**Table 3** | Values to be combined for the simulations

| Parameter | Value 1 | Value 2 | Value 3 |
|---|---|---|---|
| **Ram Speed** ($mm/s$) | 35 | 40 | 45 |
| **Melt Temperature** (°C) | 260 | 270 | 280 |
| **Venting** ($\mu m$) | 1.5 | 3 | 4.5 |

**Figure 12** | View of the complete meshed part **Picture from Moldflow Insight 2017**

# 5 Validation and results

Validation is only performed at meso scale due to time concerns that made it impossible to include data for the micro scale validation. The process of validating the model is done by comparing the values obtained from simulations to values from the injection molding experiments. To make a solid comparison, not only completely injected pieces were studied. Instead, a short-shot technique was used.

The term short-shot refers to a partial filling of the mold during the injection process. Short-shots can be obtained intentionally, when the process is deliberately stopped before its end, or unwittingly, caused by problems such as low injection pressures or frozen melt along the front flow. In this case, short-shots were intentionally provoked by limiting the injection stroke. Using the short-shots technique, it is possible to obtain data for different steps of the filling process, having more data to compare the model with and also making it possible to observe the filling pattern as it evolves.

The short-shots were injected stopping the stroke at four different positions: 8 $mm$; 12 $mm$; 16 $mm$ and 20 $mm$. The 8 $mm$ shot corresponds to the completely injected piece. The injection machine was programmed for every shot with ram speed and melt temperature values equivalent to the *Value 2* parameters in **Table (3)**. Different pieces for every injection shot were given together with data covering the real injection conditions registered by the injection machine sensors. As it is not possible to simulate short-shots in Moldflow, data from the simulations was obtained by simulating the filling of the whole part and extracting the values for certain time or ram position according to the value of the shot.

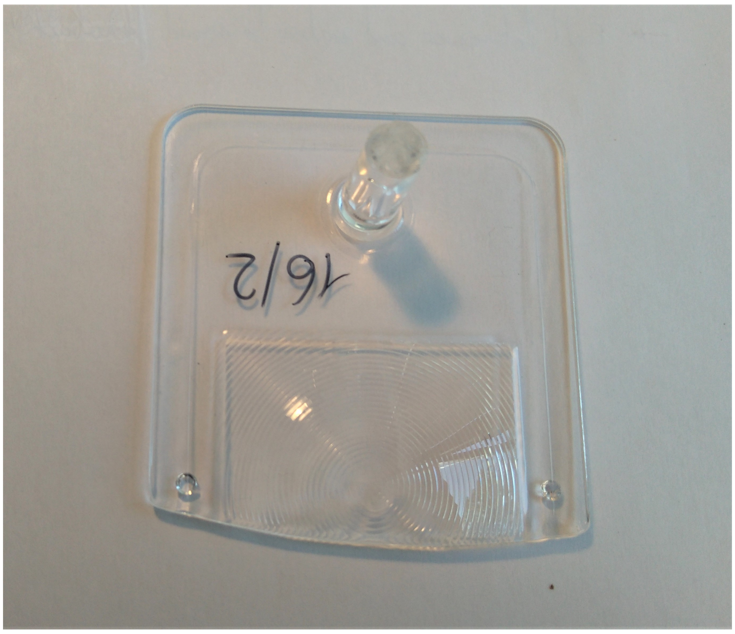

**Figure 13** | Picture of a 16 $mm$ shot piece. **Photograph by the author**

This section includes comparisons between simulated values, data from the injection machine and nominal values from the piece design. Parameters to be compared include Final Time of the short shots, final position, pressure at the injection point, mass of the pieces, and measurements of the macroscopic features among others.

Simulations were performed following the procedure explained in section **4.3 Modelling experiments.** After executing the 27 simulations and analyzing the data extracted from them, it was found that venting had no impact in the parameters being observed. This means that for the same ram speed and melt temperature, different venting values would obtain the same results.

An explanation to this unexpected outcome could be that the increase in value for the simulation iterations would not be large enough to cause any change in the results, although this theory has not been confirmed. Results for venting iterations are omitted to avoid unnecessary repetition.

## 5.1 Injection parameters comparison

As it has been explained before, venting, ram speed and melt temperature were considered as variables in the simulation. Other injection parameters can be studied as variables, being used for validating the model. This parameters are: final time of the injection process, final ram position and pressure at the injection point at the end of the injection shot. Each variable is compared with the real value for each shot and differences are discussed.

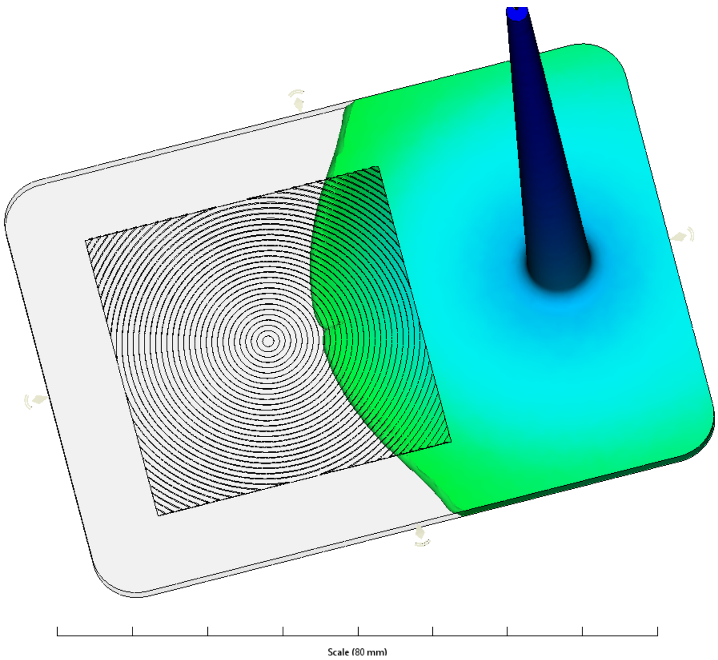


**Figure 14** | Picture of the filling analysis simulation. **Image from Moldflow Insight 2017**

### 5.1.1 Final time deviation

Influence of ram speed and temperature on the final time is studied in this point.The percentage deviation between the simulated values and the machine data is obtained and used to compare how melt temperature and ram speed affect process timing. As it can be observed on the next graphic, the tendency is to have lower deviations when simulating using the injection conditions that were used in the machine.

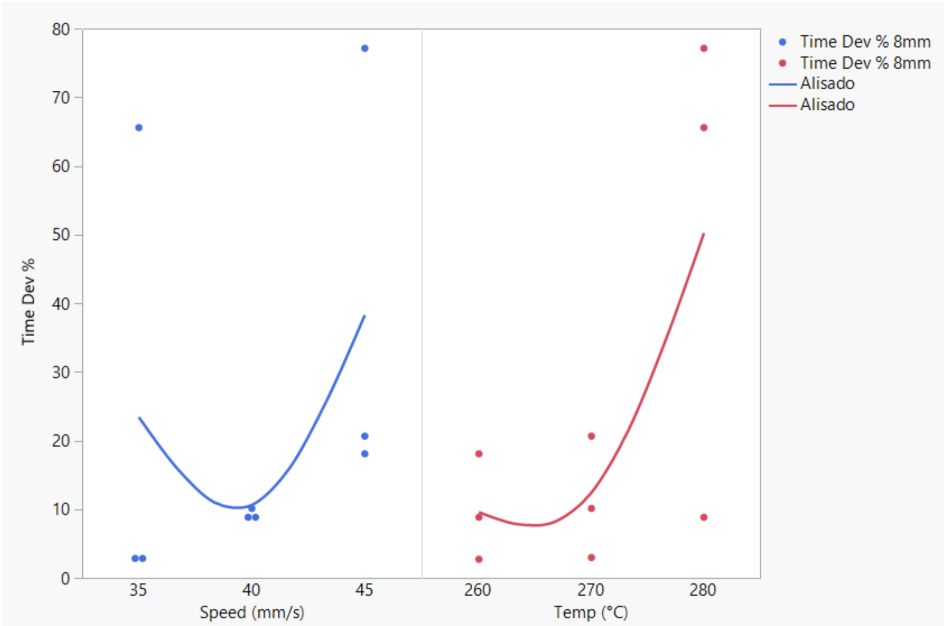


**Figure 15** | % Deviation of time versus ram speed and melt temperature for the 8 $mm$ shot. **Chart produced in JMC**

A curious phenomenon is observed from this graphs. While changing the Ram speed maintaining a constant temperature final time deviates in a predictable way, doing the opposite leads in non constant variation on the final time. If data from 6 is observed carefully, it is possible to deduce that temperature at 280 °C causes the process to be much faster. This seems to be true for 35 and 45 $mm/s$ ram speed, but it is not the case with the 40 $mm/s$ stroke, as temperature seems to have nearly no impact on it. The deviation between nominal speed results and reality is of around 10%.

For the short-shots, the trend seems to be the same, but for the shortest ones (16 $mm$ and 20 $mm$) a huge increase in deviation is observed when simulating using the injection machine conditions. This can be observed in the next figure.

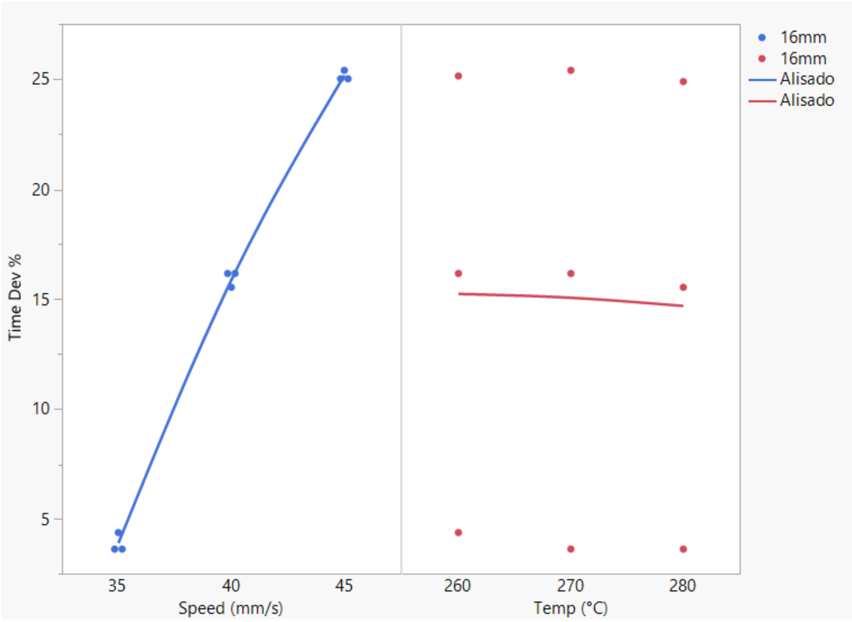


**Figure 16** | % Deviation of time versus ram speed and melt temperature for the 16 $mm$ shot. **Chart produced in JMC**

For the short-shots the change in temperature seems to have nearly no impact for any constant speed. The change of speed maintaining temperature causes a regular increase of the final time deviation. As it has been mentioned before, the nominal injection conditions deviate more in this short-shots. The lower deviations are for 35 $mm/s$ ram speed, being the deviation quite similar to those of the 8$mm$ shot.

### 5.1.2 Final position deviation

The effect of ram speed and melt temperature can be observed in the next figure for the 8 $mm$ shot. At first glance, it can be said that the tendency is the same as with the time deviation, as deviation tends to be lower when using nominal injection conditions.

Temperature seems to have not a huge impact in the results, but the truth is that using 280 °C as melt temperature can dramatically affect the results. The combination of this temperature with injection speeds different than 40 $mm/s$ causes an enormous deviation. When observing data from **Table (6)** one can realize that, except for combinations using 280 °C as melt temperature, position deviation seems to be quite stable at between 17% and 20%

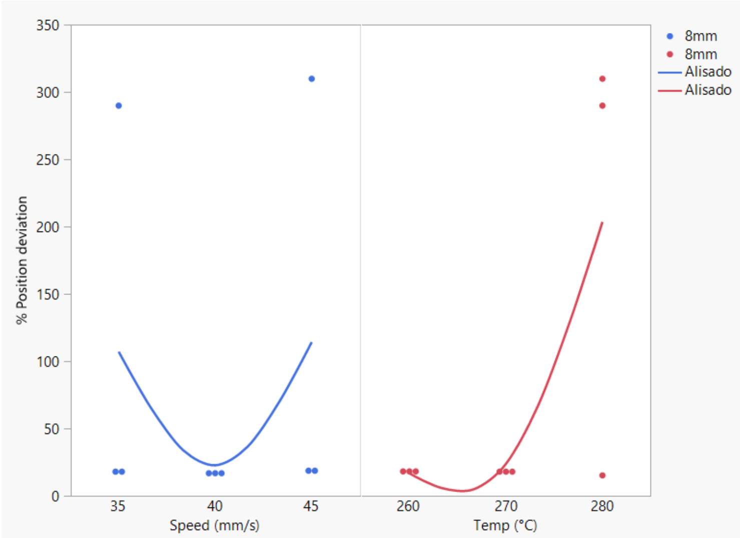


**Figure 17** | % Deviation of position versus ram speed and melt temperature for the 8 $mm$ shot. **Chart produced in JMC**

When observing the short shots, the huge impact of temperature in the final position deviation seems to vanish. Instead, much more constant discrepancies are obtained. The deviation seems to be lower the lowest the shot. This could be caused by the sensors of the machine, as there's the possibility of theme gaining precision when measuring shorter distances. An example of this, statements can be easily observed in the next figure.

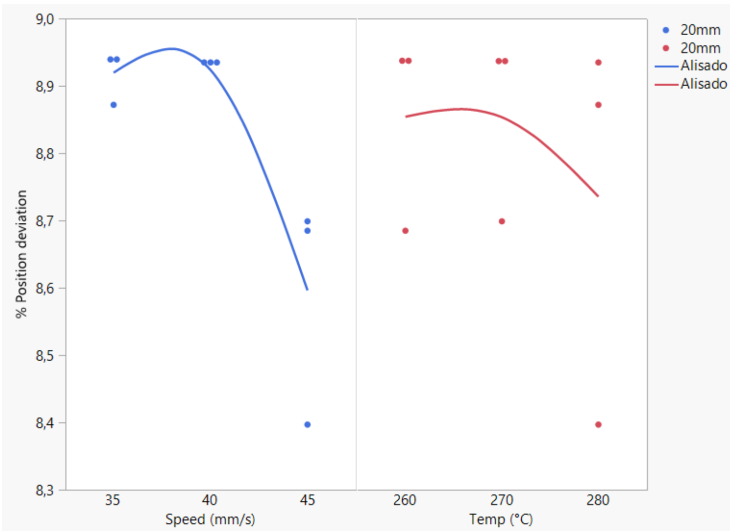


**Figure 18** | % Deviation of position versus ram speed and melt temperature for the 20 $mm$ shot. **Chart produced in JMC**

This chart can mislead the reader, as it could seem that 40 $mm/s$ speed and 270 °C do not lead to the lowest deviations. This has no relevance on the overall validation, as the values deviate so little in this conditions that the effect is only caused by the scale of the graph.

### 5.1.3 Pressure at the injection point

The third and last injection parameter which behaviour is to be observed is the pressure at the injection point. Something to observe with this parameter is that under any injection condition, pressure at the injection point remains constant. The value of the pressure is always 200 $MPa$ and deviates by 43.8% from the 355,68 $MPa$ measured by the injection machine.

For the short-shots, it is found that pressure is really influenced by changes in the melt temperature or ram speed, but it is done so within a pattern.

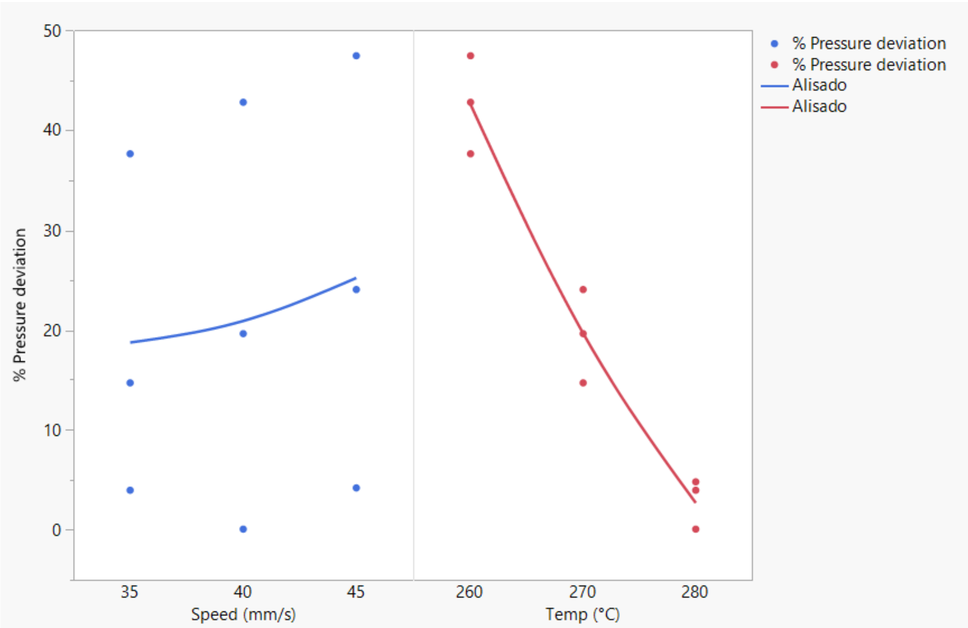


**Figure 19** | % Deviation of pressure versus ram speed and melt temperature for the 20 $mm$ shot. **Chart produced in JMC**

It is to be mentioned, that in this short-shot, the 280 °C temperature seems to be the less deviant from the injection machine measurements. However, this is not the case for the other shots. Even not allways having the lowest deviation, 40 $mm/s$ and 270 °C is the most consistent over all the conditions, with fewer variations on its deviation for different shots.

## 5.2 Mass comparaison

Mass is an easy to compare value that can also provide information on how accurate the model is. It is a good reference for validating the model at a macroscopic scale, as a triple comparison can be done.

The 8 $mm$ shot pieces are compared with the simulated value of the mass and with the effective nominal value of the mass, which is the theoretical value of the mass taking into account volumetric shrinkage of the piece.

### 5.2.1 Effective nominal value and measured value

The effective nominal value of the mass is defined by the equation below, where $V_n$ is the nominal volume obtained from the CAD model, $\Delta(V)$ is the volumetric shrinkage, obtained from the simulations and $\rho$ the density of the material.

$$V_{ef} = V_n \cdot \Delta V \cdot \rho \tag{1}$$

Applying the values to solve the equation, the effective volume is:

$$V_{ef} = 13.291 cm^3 \cdot 0.97 \cdot 1.01 g \cdot cm^{-3} = 13.2 g$$

The mass from the 8 $mm$ pieces measured with the scale is $13.68 \pm 0.001 g$ this leads to a deviation between theme of 4.8%. Higher real mass could mean that more plastic than expected is beeing injected in the mold.

Comparison whit the simulated results has a lower deviation, moving between 2% and 3% depending on the injection conditions. For an easy view of the results it is included the next graphic.

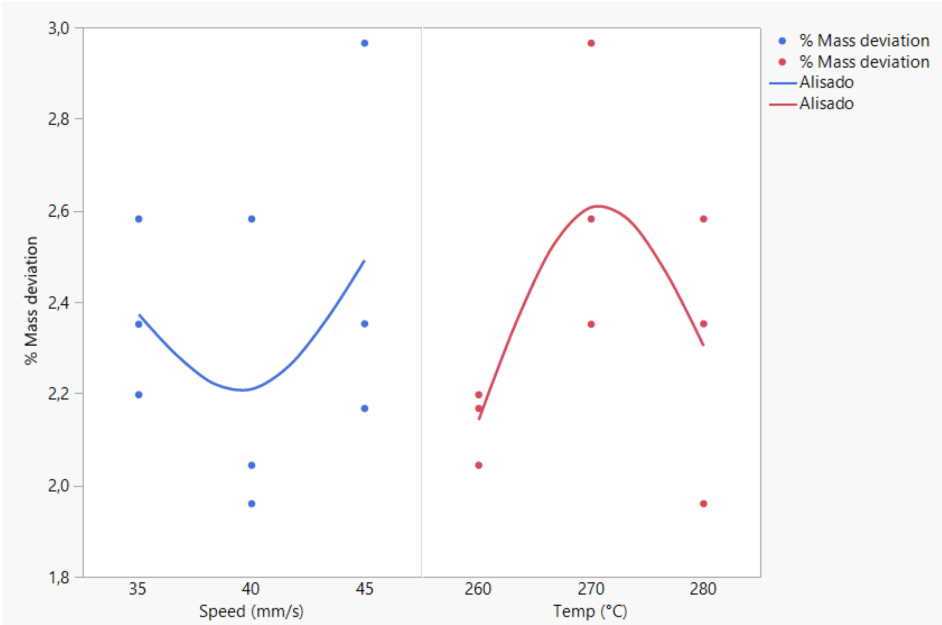


**Figure 20** | % Deviation of mass versus ram speed and melt temperature. **Chart produced in JMC**

### 5.2.2 Simulated Values

The short shots are compared using the simulated mass values and the weight from the partially completed pieces. The same was done with the 8mm shot. Values for the mass can be consulted in the appendix. From that tables, it is also possible to see that Deviation increases the shorter the shot is. This could mean that Moldflow systematically underestimates the volume of plastic being injected at the firsts stages of injection. This deviation is diminished on the longer shots, so the software starts injecting the right amount of material at some point during the simulation.

Even tough, mass is simulated with high accuracy levels, having a deviation under 10% for every shot. Interestingly, for the 8mm shot, the deviation trend is nearly the same as when comparing with the effective nominal value of the piece as it can be observed in next figure.

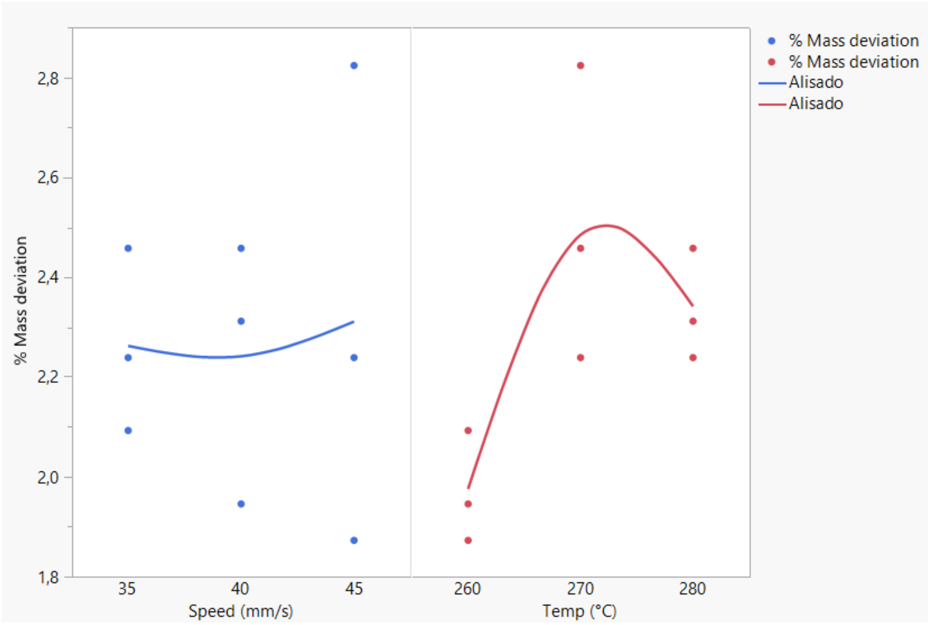


**Figure 21** | % Deviation of mass versus ram speed and melt temperature for the 8 $mm$ shot. **Chart produced in JMC**

For the reader to see how the deviation increases for the shortest shots, the deviation chart of the 20 $mm$ shot is included above. As it can be seen, the distribution of the dots becomes wider and the previous trend can not be observed.

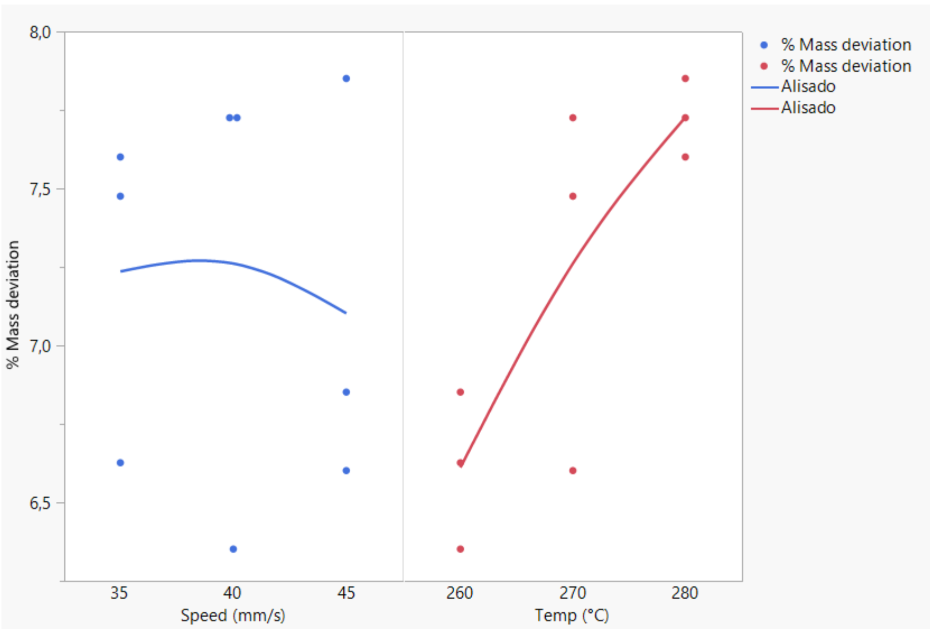


**Figure 22** | % Deviation of mass versus ram speed and melt temperature for the 8 $mm$ shot. **Chart produced in JMC**

## 5.3 Geometrical comparison

On this section no comparisons between the simulated results and the real values are performed. The length, thickness, width and diameter of the bottom of the sprue are compared with the nominal values.

The intention behind this juxtaposition of values is to ensure that the pieces are correctly replicated. In other words, that the mold is producing pieces following the requirements stated by the designer. For doing so, it is needed to compare as much values as possible, measuring a large quantity of features from the piece. Only 8mm shot pieces were measured as it is to expect from others not to appropriately replicate the mould as they are not completed yet.

Some drawbacks for achieving this were found when trying to use the optical CMM. The machine would not obtain repeatable values due to the not so straight edges that were intended to be measured on the piece. As a solution, the piece was measured using a caliper and a micrometer.

In the next tables we can see nominal values for the features measured and measurements from the pieces. All measurements are in $mm$ if not explicitly said.

**Table 4** | Nominal values of the measured features

| Feature | Value | Units |
|---|---|---|
| **Width** | 60 | mm |
| **Lenght** | 85 | mm |
| **Diameter** | 8.6 | mm |
| **Thickness** | 2 | mm |

**Table 5** | Measured Values

| Feature | Value |
|---|---|
| **Width** | $59.763 \pm 0.033 mm$ |
| **Lenght** | $84.6 \pm 0.034 mm$ |
| **Diameter** | $8.599 \pm 0.301 mm$ |
| **Thickness** | $2.07 \pm 0.030 mm$ |

Over all, the pieces seem to be correctly replicating the model, so no differences should be caused because of injection discrepancies.

# 6 Conclusions

Obtaining a three dimensional model of injection molded Fresnel lenses is a challenging process due to the micro-structure of the pieces. After trying different methods, a mesh that provides good resolution has been built. The resolution is only adequate around ridge 14, in a really small area. This is enough for validating the model, but there is room for improvement. More computational power and time would be needed, in order to achieve a mesh with good resolution all over the piece.

Simulations were planed combining different injection conditions to see how they affected the final results. This has been analyced in depth on this report, making it possible to confirm that the lowest and most consistent deviations are obtained when simulating using the temperature and ram speed used in the injection machine.

An analysis has been performed in order to validate the process, comparing real values with others from the simulations. Over all, the model can be considered valid within an accuracy that is within reasonable limits. All the measurements and the data used in the treatment of the simulation were obtained from Moldflow or using adequate measuring equipment.

No validation of the model could be done at micro-scale due to time concerns. This is work to be resumed, as the model should be valid both at meso and micro scale.

Knowledge in injection molding for high precision manufacturing was acquired. It was also learned how to use simulation tools for injection molding processes and how to create and validate a three dimensional model of the process.

# References


[1] B. A. Anicin et Al. Fresnel lenses. *Am. J. Phys*, 57:312–316, 1989.

[2] H. Nishihara and T. Suhara. Micro fresnel lenses. *E. Wolf Progress in Optics - Elsevire Science Publisher B.V.*, 24, 1987.

[3] Arthur Davis. Fresnel lens solar concentrator derivations and simulations. *Proceedings of SPIE - The International Society for Optical Engineering*, 8129, 2011.

[4] CM Lin and HK Hsieh. Processing optimization of fresnel lenses manufacturing in the injection molding considering birefringence effect. *Mycrosystem Technologies*, 23:5689, 2017.

[5] J. Shoemaker. *Moldflow Design Guide: A Resource for Plastics Engineers.* Carl Hanser Verlag GmbH Co. KG, 2006.

[6] Danilo Quagliotti P. Parenti M. Annoni Dario Loaldi, Matteo Calaon and Guido Tosello. Zero defects manufacturing in injection compression molding of polymer fresnel lenses. *N.d.*, 2018.

[7] T. Takayama H. Suzuki and H. Ito. international journal of modern physics: Conference series. *N.d.*, 06:563, 2012.

[8] Sabrina S. Jedlicka Ali A. Rajhi and John P. Coulter. Moldflow optimization of micro-cavities filling during injection molding process. *ANTEC 2018 conference proceedings, Society of Plastics Engineers (SPE)*, 2018.

[9] Matteo Calaon Dario Loaldi, Danilo Quagliotti and Guido Tosello. Modelling the filling behavior of micro structured plastic optical components. *Worl Conference on Micro and Nano Manufacturing*, 2019.

[10] Terje Tofteberg and Erik Andreassen. Multiscale simulations of the injection moulding of a diffractive optical element. *N.d.*, 2015.

[11] Editor Autodesk. *Autodesk Moldflow Insight Advanced Flow Practice Manual.* Autodesk, 2016.

[12] K. Talwar et al. Three-dimensional simulation of plastic injection moulding. *ANTEC 1998 conference proceedings, Society of Plastics Engineers (SPE)*, 1998.

[13] ZEON ® official website. cyclo olefin polymer (cop) - zeonex ®. Last accessed 9 June 2019.

# A Appendix: Complete data tables

**Table 6** | Results from 8 $mm$ shot simulation and real value from injection experiments.

| | | | | | | | | | | **Real** |
|---|---|---|---|---|---|---|---|---|---|---|
| **Speed (mm/s)** | **35** | **35** | **35** | **40** | **40** | **40** | **45** | **45** | **45** | **39.282** |
| **Temp (°C)** | **260** | **270** | **280** | **260** | **270** | **280** | **260** | **270** | **280** | **270** |
| **Final Time (s)** | 0.800 | 0.802 | 0.268 | 0.710 | 0.700 | 0.710 | 0.638 | 0.618 | 0.178 | **0.779** |
| **Final Position (mm)** | 8.129 | 7.986 | 26.620 | 8.066 | 8.000 | 7.870 | 8.021 | 8.190 | 27.990 | **6.827** |
| **Pressure (MPa)** | 200 | 200 | 200 | 200 | 200 | 200 | 200 | 196.082 | 200 | **355.86** |
| **Mass (g)** | 13.39 | 13.37 | 13.34 | 13.41 | 13.34 | 13.36 | 13.42 | 13.29 | 13.37 | **13.68** |
| **Dev Time (s)** | 0.021 | 0.023 | 0.511 | 0.069 | 0.079 | 0.069 | 0.141 | 0.161 | 0.601 | |
| **Dev Position (mm)** | 1.302 | 1.159 | 19.793 | 1.239 | 1.173 | 1.043 | 1.194 | 1.363 | 21.163 | |
| **Dev Pressure (Mpa)** | 155.86 | 155.86 | 155.86 | 155.86 | 155.86 | 155.86 | 155.86 | 159.778 | 155.86 | |
| **Dev Weight (g)** | 0.286 | 0.306 | 0.336 | 0.266 | 0.336 | 0.316 | 0.256 | 0.386 | 0.306 | |
| **Time Dev %** | 2.742 | 2.986 | 65.597 | 8.858 | 10.141 | 8.858 | 18.100 | 20.668 | 77.150 | |
| **Position Dev %** | 19.078 | 16.978 | 289.922 | 18.144 | 17.182 | 15.272 | 17.491 | 19.965 | 309.990 | |
| **Pressure Dev %** | 43.798 | 43.798 | 43.798 | 43.798 | 43.798 | 43.798 | 43.798 | 44.899 | 43.798 | |
| **Weight Dev %** | 2.093 | 2.239 | 2.458 | 1.946 | 2.458 | 2.312 | 1.873 | 2.824 | 2.239 | |

**Table 7** | Results from 12 $mm$ shot simulation and real value from injection experiments.

| | | | | | | | | | | **Real** |
|---|---|---|---|---|---|---|---|---|---|---|
| **Speed (mm/s)** | **35** | **35** | **35** | **40** | **40** | **40** | **45** | **45** | **45** | **39.282** |
| **Temp** (°C) | **260** | **270** | **280** | **260** | **270** | **280** | **260** | **270** | **280** | **270** |
| **Final Time (s)** | 0.680 | 0.680 | 0.687 | 0.598 | 0.598 | 0.598 | 0.535 | 0.533 | 0.533 | **0.66** |
| **Final Position (mm)** | 12.200 | 12.200 | 11.954 | 12.080 | 12.080 | 12.080 | 11.940 | 12.003 | 11.997 | **10.641** |
| **Pressure (MPa)** | 46.915 | 39.104 | 32.724 | 48.673 | 40.781 | 34.115 | 50.258 | 42.286 | 35.521 | **34.083** |
| **Mass (g)** | 9.960 | 9.940 | 9.920 | 9.990 | 9.900 | 9.890 | 9.920 | 9.930 | 9.910 | **12.55** |
| **Dev Time (s)** | 0.020 | 0.020 | 0.027 | 0.062 | 0.062 | 0.062 | 0.125 | 0.127 | 0.127 | |
| **Dev Position (mm)** | 1.559 | 1.559 | 1.313 | 1.439 | 1.439 | 1.439 | 1.299 | 1.362 | 1.356 | |
| **Dev Pressure (Mpa)** | 12.832 | 5.021 | 1.359 | 14.590 | 6.698 | 0.032 | 16.175 | 8.203 | 1.438 | |
| **Dev Weight (g)** | 2.589 | 2.609 | 2.629 | 2.559 | 2.649 | 2.659 | 2.629 | 2.619 | 2.639 | |
| **Time Dev %** | 3.030 | 3.030 | 4.097 | 9.394 | 9.394 | 9.394 | 18.991 | 19.202 | 19.180 | |
| **Position Dev %** | 14.651 | 14.651 | 12.335 | 13.523 | 13.523 | 13.523 | 12.210 | 12.800 | 12.738 | |
| **Pressure Dev %** | 37.649 | 14.730 | 3.987 | 42.807 | 19.653 | 0.093 | 47.459 | 24.067 | 4.220 | |
| **Weight Dev %** | 20.630 | 20.789 | 20.949 | 20.391 | 21.108 | 21.188 | 20.949 | 20.869 | 21.028 | |

**Table 8** | Results from 16 $mm$ shot simulation and real value from injection experiments.

| | | | | | | | | | | Real |
|---|---|---|---|---|---|---|---|---|---|---|
| **Speed (mm/s)** | **35** | **35** | **35** | **40** | **40** | **40** | **45** | **45** | **45** | **39.282** |
| **Temp** (°C) | **260** | **270** | **280** | **260** | **270** | **280** | **260** | **270** | **280** | **270** |
| **Final Time (s)** | 0.568 | 0.572 | 0.572 | 0.498 | 0.498 | 0.502 | 0.445 | 0.443 | 0.446 | **0.594** |
| **Final Position (mm)** | 16.120 | 15.964 | 15.965 | 16.080 | 16.080 | 15.931 | 15.992 | 16.060 | 15.924 | **14.438** |
| **Pressure (MPa)** | 43.054 | 35.948 | 30.068 | 44.602 | 37.421 | 31.461 | 46.043 | 38.761 | 32.725 | **35.191** |
| **Mass (g)** | 9.960 | 9.940 | 9.920 | 9.990 | 9.900 | 9.840 | 9.920 | 9.930 | 9.910 | **10.32** |
| **Dev Time (s)** | 0.026 | 0.022 | 0.022 | 0.096 | 0.096 | 0.092 | 0.149 | 0.151 | 0.148 | |
| **Dev Position (mm)** | 1.682 | 1.526 | 1.527 | 1.642 | 1.642 | 1.493 | 1.554 | 1.622 | 1.486 | |
| **Dev Pressure (Mpa)** | 7.863 | 0.757 | 5.123 | 9.411 | 2.230 | 3.730 | 10.852 | 3.570 | 2.466 | |
| **Dev Weight (g)** | 0.360 | 0.380 | 0.400 | 0.330 | 0.420 | 0.480 | 0.400 | 0.390 | 0.410 | |
| **Time Dev %** | 4.377 | 3.625 | 3.632 | 16.162 | 16.162 | 15.535 | 25.146 | 25.401 | 24.892 | |
| **Position Dev %** | 11.650 | 10.567 | 10.577 | 11.373 | 11.373 | 10.341 | 10.760 | 11.233 | 10.291 | |
| **Pressure Dev %** | 22.343 | 2.150 | 14.557 | 26.742 | 6.337 | 10.600 | 30.837 | 10.145 | 7.008 | |
| **Weight Dev %** | 3.486 | 3.680 | 3.873 | 3.195 | 4.067 | 4.649 | 3.873 | 3.777 | 3.970 | |

**Table 9** | Results from 10 $mm$ shot simulation and real value from injection experiments.

| | | | | | | | | | | **Real** |
|---|---|---|---|---|---|---|---|---|---|---|
| **Speed (mm/s)** | **35** | **35** | **35** | **40** | **40** | **40** | **45** | **45** | **45** | **39.282** |
| **Temp** (°C) | **260** | **270** | **280** | **260** | **270** | **280** | **260** | **270** | **280** | **270** |
| **Final Time (s)** | 0.455 | 0.455 | 0.455 | 0.398 | 0.398 | 0.398 | 0.355 | 0.355 | 0.356 | **0.472** |
| **Final Position (mm)** | 20.081 | 20.081 | 20.068 | 20.080 | 20.080 | 20.080 | 20.034 | 20.037 | 19.981 | **18.433** |
| **Pressure (MPa)** | 32.819 | 27.436 | 27.436 | 40.616 | 34.143 | 28.680 | 41.863 | 35.377 | 30.841 | **35.252** |
| **Mass (g)** | 7.478 | 7.410 | 7.400 | 7.500 | 7.390 | 7.390 | 7.460 | 7.480 | 7.380 | **8.01** |
| **Dev Time (s)** | 0.017 | 0.017 | 0.017 | 0.074 | 0.074 | 0.074 | 0.117 | 0.117 | 0.116 | |
| **Dev Position (mm)** | 1.648 | 1.648 | 1.635 | 1.647 | 1.647 | 1.647 | 1.601 | 1.604 | 1.548 | |
| **Dev Pressure (Mpa)** | 2.433 | 7.816 | 7.816 | 5.364 | 1.109 | 6.572 | 6.611 | 0.125 | 4.411 | |
| **Dev Weight (g)** | 0.531 | 0.599 | 0.609 | 0.509 | 0.619 | 0.619 | 0.549 | 0.529 | 0.629 | |
| **Time Dev %** | 3.638 | 3.637 | 3.561 | 15.678 | 15.678 | 15.678 | 24.830 | 24.842 | 24.580 | |
| **Position Dev %** | 8.940 | 8.939 | 8.872 | 8.935 | 8.935 | 8.935 | 8.685 | 8.699 | 8.397 | |
| **Pressure Dev %** | 6.902 | 22.172 | 22.172 | 15.215 | 3.146 | 18.642 | 18.753 | 0.354 | 12.513 | |
| **Weight Dev %** | 6.627 | 7.476 | 7.601 | 6.352 | 7.726 | 7.726 | 6.852 | 6.602 | 7.851 | |

**Department of Mechanical Engineering**
Section of Manufacturing engineering
Danmarks Tekniske Universitet
Produktionstorvet Building 427
DK-2800 Kgs. Lyngby
Denmark
www.mek.dtu.dk
Tel: (+45) 45 25 19 16
Fax: (+45) 45 93 14 75
Email: info@mek.dtu.dk

**Escuela Técnica Superior de Ingenieria del Diseño**
Grado en Ingeniería Mecánica
**Universitat Politècnica de València**
Camino de Vera s/n, Edificio 7B
46022 València
Spain
http://www.etsid.upv.es
Tel: (+34) 96 387 70 00 Ext.71800
Fax: (+34) 963 877 189
Email: secretaria@etsid.upv.es